

GT2011-4538

REMAINING LIFE ASSESSMENT TECHNOLOGY APPLIED TO STEAM TURBINES AND HOT GAS EXPANDERS

Phillip Dowson

General Manager of Materials Engineering
Elliott Group
901 North Fourth Street
Jeannette, PA 15644, USA
Email: pdowson@elliott-turbo.com

David Dowson

Service Engineer (Repairs)
Elliott Group
901 North Fourth Street
Jeannette, PA 15644, USA
Email: ddowson@elliott-turbo.com

ABSTRACT

In today's market place, a large percentage of oil refinery, petrochemical, and power generation plants throughout the world have been trying to reduce their operation cost by extending the service life of their critical machines, such as steam turbines, beyond the design life criteria. The key ingredient in plant life extension is Remaining Life Assessment Technology. This paper will outline the Remaining Life Assessment procedures, and review the various damage mechanisms such as creep, fatigue, creep-fatigue and various embrittlement mechanisms that can occur in these machines. Also highlighted will be the various testing methods for determining remaining life or life extension of components such as high precision STR (Stress Relaxation Test), which determines creep strength, and CDR (Constant Displacement Rate) Test, which evaluates fracture resistance. Other tests such as replication/microstructure analysis and toughness tests will also be reviewed for calculating the remaining life or life extension of the components. Use of the latest computer software will also be highlighted showing how creep-life, fatigue-life and creep/fatigue-life calculations can be performed. Also shown will be an actual life extension example of a hot gas expander performed in the field.

INTRODUCTION

In recent years, from oil refinery to petrochemical and power generation industries, more and more plants throughout the world are facing a common issue – aging turbines, usually over 30 years old. Questions bearing in managers' mind are what is the machine condition and whether they can be continually operated (if yes, how long). The answer is significant not only for safety concern but also for cost reduction, especially with today's limited budget. Therefore, there is an increasingly strong desire for the engineering aftermarket service to perform "remaining life assessment" of steam turbines and hot gas expanders.

Remaining life assessment is to use metallurgical and fracture mechanics methodologies to predict the remaining life of structures and components that have been in service for an extended period of time, usually close to or beyond the designed life. Traditionally, if parts are found with material degradations or damages during an overhaul, they might be scrapped and replaced for risk-free consideration; even though they might have some useful life.

Remaining life assessment offers a possible tool to estimate the useful remaining lifetime and avoid premature scrapping of the parts. So remaining life assessment is considered to be an attractive method/process for cost reduction and reduction down-time.

In evaluating the failure criteria or remaining life, one needs to understand the various failure mechanisms that can occur. In turbomachinery components, the failure criteria can be governed by one or a combination of the following failure mechanisms:

- Fatigue – high cycle or low cycle
- Corrosion / Corrosion Fatigue
- Stress Corrosion Cracking (SCC)
- Erosion – solid particle or liquid impingement
- Erosion Corrosion
- Creep Rupture / Creep Fatigue
- High temperature corrosion/embrittlement
- Mechanical (foreign objective) Damage

However, in remaining life assessment, usually only those mechanisms depending on temperature and time are taken into account. For example, for turbine casing, engineers usually focus on thermal stress-induced low cycle fatigue, creep rupture, and tempering embrittlement cracking. These failures usually are slow processes, therefore, can be assessed and forecasted by examining the warning evidences in the material.

Countless works have been done to study the behaviors of fatigue crack initiation/propagation and creep or embrittlement rupture in steels and alloys. Scientists and engineers have reached such a level that, by knowing the flaw size or microstructure deterioration/damage, one can theoretically calculate and predict the remaining lifetime of the parts, based on the knowledge of the material properties, operating variables/environment and understanding of the stress distributions.

CREEP RUPTURE AND STRESS RUPTURE

Evidence of creep damage in the high temperature regions of blade attachment areas of rotors has been observed in some instances (Bush, 1982). The rim stresses and metal temperature at these locations are assessed against the creep rupture data for that particular grade of steel/or material. Traditionally one has used a Larson-Miller (LM) plot of the type shown in Figure 1.

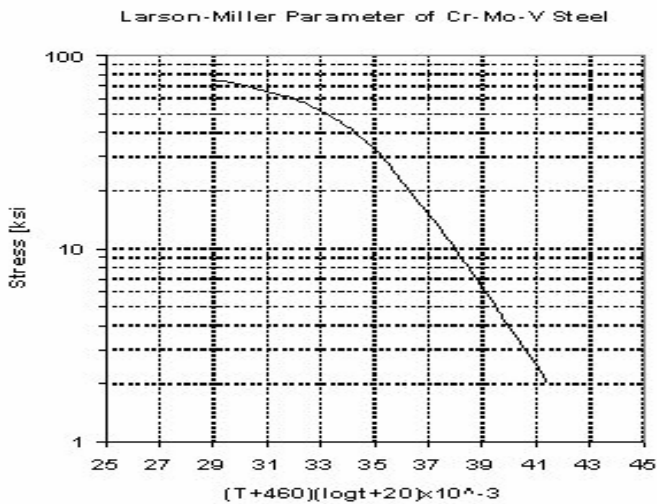


Figure 1. Larson-Miller Curve of Cr-Mo-V Alloy Steel (ASTM A470 Class 8).

The degree of safety margin depends on the user and what lower bound design curve is applied. Since these curves are based upon the chemistry, variation in chemistry for a particular grade can have an effect on the Larson-Miller curve. Also, Larson-Miller curves are generally based upon creep rupture tests done for 10^4 to 3×10^4 hours and very few data at 10^5 hours. Consequently, the data for longer hours are generally extrapolated. Since most of the creep rupture data is done with smooth bar specimens, the effect of notch ductility at long-term service has not been done. Short term notched bars tests may fail to predict the onset of notch sensitivity. Notch sensitivity is not an inherent property but depends on the temperature, stress, stress state, and strain rate. Other factors such as material cleanliness leading to hard second phase particles and environmental embrittlement can also create notch sensitivity.

In assessing remaining life of components due to creep, such as blade attachments, crack initiation is used as the criteria. However, with the emergence of cleaner steel and fracture mechanics and an increasing need to extend the life of component, application of crack growth techniques have become common in the past decade.

For crack initiation as the fracture criteria, history-based calculation methods are often used to estimate life.

Methods for Crack Initiation Due To Creep

For the analytical method, one must have accurate operating history of the components, which may consist of temperature, applied loads, changes in operation, such as shut downs or variation in speed or pressure. A simplistic estimation of the creep life expended can be made by assessing the relaxed long-term bore stresses and rim-stresses against the standard rupture data using the life fraction rule. The life fraction rule (LFR) states that at failure:

$$\sum \frac{t_i}{t_{ri}} = 1 \quad (1)$$

where:

t_i is the time spent at a given stress and temperature and t_{ri} is the rupture life for the same test conditions.

This rule was found to work well for small changes in stress and temperature especially for CrMoV rotor steel. However, for stress variations, the actual rupture lives were lower than the predicted values. Consequently, the LFR is generally valid for variable-temperature conditions as long as changing creep mechanisms and environmental interaction do not interfere with test results. However, the possible effect of material ductility on the applicability of the LFR needs to be investigated.

Non-Destructive Techniques

Conventional non-destructive evaluation (NDE) techniques fail to detect incipient damage which can be a precursor to crack initiation and subsequent rapid failure. However, there are other NDE techniques that have been developed for estimating the life consumption. These include microstructural techniques and hardness based techniques.

Metallographic Examination

Metallographic techniques have been developed that can correlate changes in the microstructure and the onset of incipient creep damage, such as triple point cavitation at the grain boundaries. For this technique, measurements by replication technique are taken on crack sensitive areas that are subjected to the higher temperatures and stresses. These areas are generally indicated by experience and analysis of previous damages.

The creep damage measured by replication is classified into four damage stages:

- Isolated cavities (A)
- Oriented cavities (B)
- Macrocracks (linking of cavities) (C)
- Formation of macrocracks (D)

Figure 2 shows the location of the four stages on the creep strain/exposure time curve (Neubauer and Wadel, 1983).

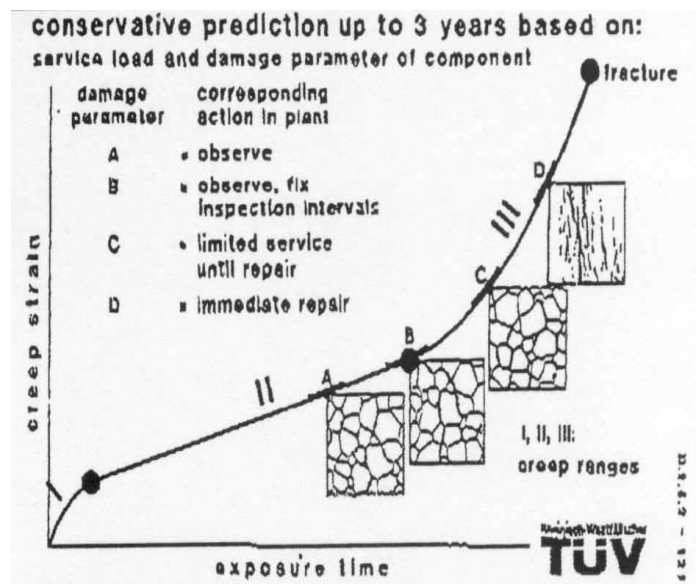


Figure 2. Replicas for Remaining Life Assessment.

In applying this approach Neubauer and Wadel (1983) classified the stages into five stages which are Undamaged, Stage A, Stage B,

Stage C, and Stage D. These stages corresponded roughly to expended life fractions (t/t_r) values of 0.27, 0.46, 0.65, 0.84 and 1 respectively using the conservative lower bound curve. Consequently, the remaining life can be calculated using the relationship as shown in Equation (2):

$$t_{rem} = t \left(\frac{t_r}{t} - 1 \right) \quad (2)$$

where:

t is the service life expended and t_r is the rupture life.

For undamaged material and damaged stages A, B, and C, the remaining life was found to be approximately $2.7t$, $1.17t$, $0.54t$, and $0.19t$ respectively. Then by applying a safety factor of 3 to the calculations, the safe re-inspection intervals will become $0.9t$, $0.4t$, $0.18t$, and $0.06t$, respectively. This approach has been developed and implemented in the power generation industry (Viswanathan and Gehl, 1991). It was found to give increased inspection intervals as compared to the Neubauer and Wadel (1983) approach, as shown in Table 1.

Table 1. Suggested Re-inspection Intervals for a Plant with 30 Years of Prior Service.

Damage Classification	Inspection Interval (Years)	
	Wedel-Neubauer	EPRI-APTECH
Undamaged	5	27
A. Isolated Cavities	3	12
B. Oriented Cavities	1.5	5.4
C. Linked Cavities (Microcracks)	0.5	1.8
D. Macrocracks	Repair Immediately	Based on fracture mechanics

This approach has been applied by several utilities and realized significant savings in inspection costs. Other investigations indicate that there are wide variations in behavior due to differences in grain size, ductility and impurity control (Carlton, et al. 1967). For conservatism, the authors' company adapted the Neubauer and Wadel (1983) approach and classified the five stages as follows:

1. Undamaged material: Equipment can run and be re-inspected at next shutdown.
2. Class A – Re-inspection would be three to five years.
3. Class B – Re-inspection would be one and one-half to three years.
4. Class C – Replacement or repair would be needed within six months.
5. Class D – Immediate replacement or repair would be required.

Other documents have been published that correlate the presence of cavities to creep damage. An example of this graphical representation is shown in Table 2 and Figure 3. Classes 4 and 5 should be considered in the stages of tertiary creep while Class 3 is the transition point between secondary and tertiary. The Class 2 is a representative of secondary creep, the advancement of that class depending upon the sub-classification indicated in Table 2 (Fossati-Sampietri, 2001).

Table 2. VGB Guidelines Classification

Assessment class	Structural and damage conditions
0	As received, without thermal service load
1	Creep exposed, without cavities
2a	Advanced creep exposure, isolated cavities
2b	More advanced creep exposure, numerous cavities without preferred orientation
3a	Creep damage, numerous orientated cavities
3b	Advanced creep damage, chains of cavities and/or grain boundary separations
4	Advanced creep damage, microcracks
5	Large creep damage, macrocracks

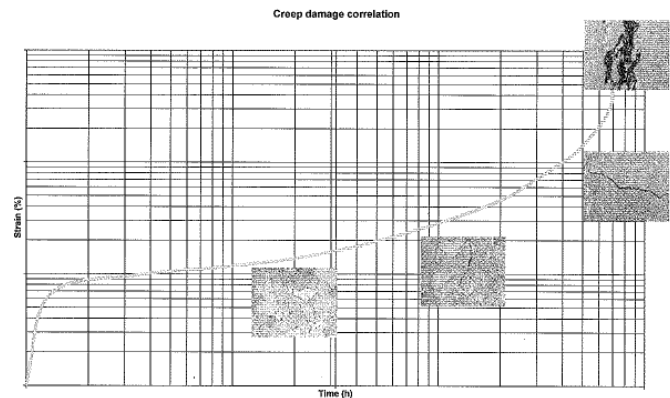


Figure 3. Example of Creep Damage Classification and Creep Curve.

Another approach is summarizing the correlation of damage level and the expanded life fraction shown in Figure 4. Fossati-Sampietri, (2001) performed a critical review of this data and other plant investigation and derived the following table correlating damage class and extended life fraction Table 3. Assumptions made for this correlation are quite conservative but results are agreement with other studies (i.e., first detection of cavities by light microscope) starts at an expected life fraction of 50 to 60%. Although the derived cavitation parameter A or A+ has been correlated to residual life assessment (life fraction) with rotor forging CrMoV steel, no other applications have been done to other components, Figure 5.

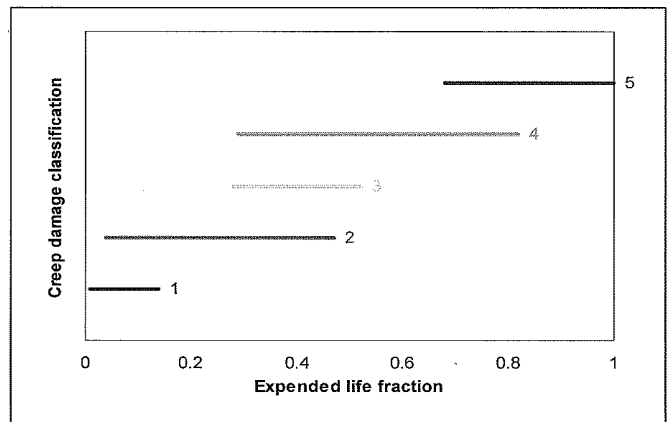


Figure 4. Creep Damage Classification and Expended Life Fraction.

Table 3. Creep Damage and Expended Life Fraction

Damage level	Expended life fraction
1	0.181
2	0.442
3	0.691
4	0.889
5	1.000

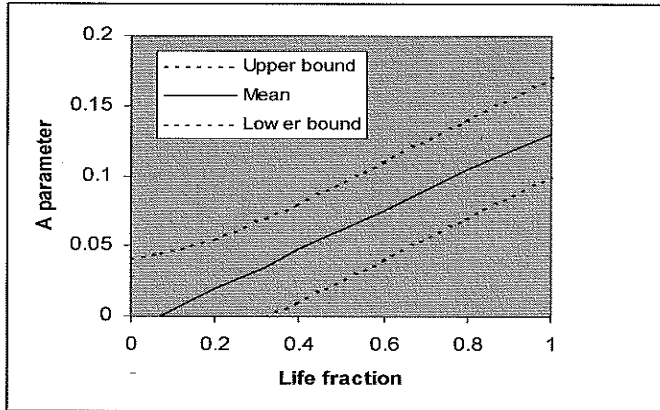


Figure 5. A-parameter and Life Fraction

Hardness Measurement

The first attempt to develop hardness as a technique to determine creep damage was by Goldhoff and Woodford (1972). In their study a good correlation was observed between room temperature hardness measured on exposed short-term creep specimens and the post exposure rupture life (Figure 6).

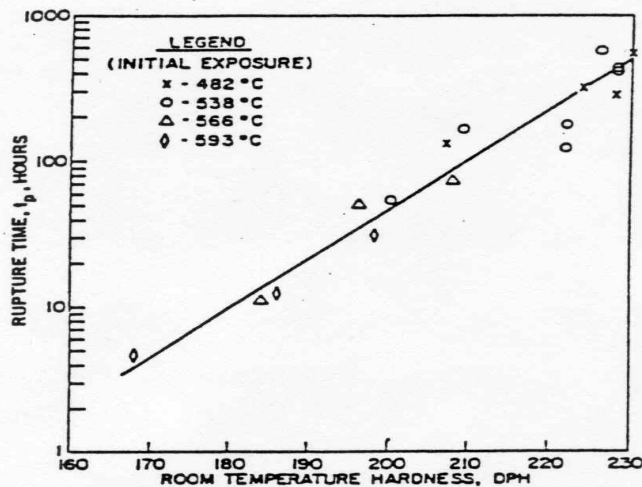


Figure 6. Correlation Between Post-Exposure Rupture Time in the Standard Test at 538°C (1000°F) and 240 MPa and Room Temperature Hardness for Cr-Mo-V Rotor Steel.

If similar calibration could be established between prior creep life expended or the remaining life fraction in the post exposure test and

the hardness values for a range of CrMoV steels, this method could be applied to estimation of remaining life. However, data of this nature are not available in sufficient quantity. Other work done by Viswanathan and Gehl (1992) showed a lot of promise where they attempted to use the hardness technique as a stress indication. They observed that the application of stress accelerated the softening process and shifted the hardness to lower parameter values compared with the case of simple thermal softening on a plot of hardness versus a modified Larson-Miller parameter (Figure 7).

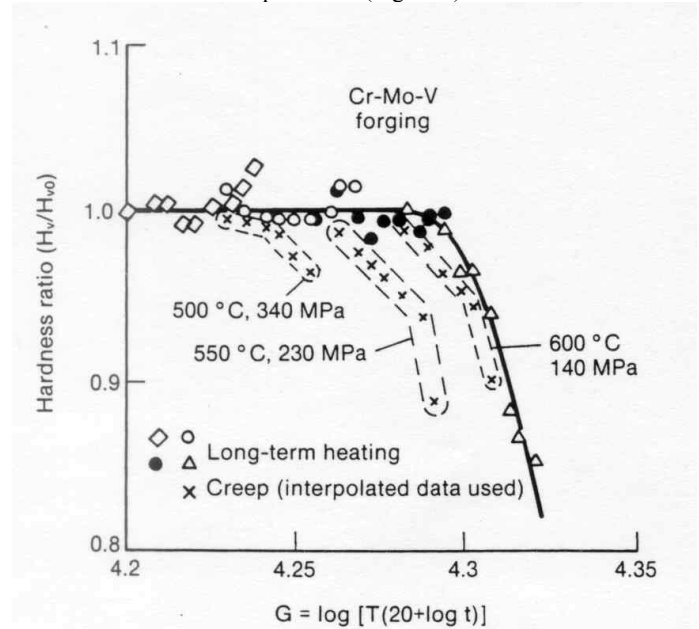


Figure 7. Plot of Hardness Ratio Versus G Parameter for Long-Term Heating and Creep of Cr-Mo-V Rotor Steel.

Destructive Techniques

Newer tests to ascertain the useful life of used and/or repaired components have been utilized by the authors' company. Design-for-performance is a recently developed methodology for evaluating the creep strength and fracture resistance of high temperature materials. Whereas the traditional approach to creep design involves long-term testing and attempts to incorporate microstructural evolution in the test measurements, the new approach aims to exclude these changes in a short time high-precision test. The test may also be used to evaluate consequences of such changes in service-exposed samples. The new methodology recognizes that separate tests are necessary to measure creep strength and fracture resistance. For creep strength, a stress versus creep rate response is determined from a stress relaxation test (SRT) and for fracture resistance a constant displacement rate (CDR) test of a notched temple specimen is performed at a temperature where the part is most vulnerable to fracture (Woodford, 1993).

However, modern approaches to repair, rejuvenation or replacement of critical components require rapid turnaround and seek accurate assessment of material performance capability. Hence there is a strong interest in accelerated testing.

The conventional creep rupture test involves an arbitrary combination of deformation processes and fracture processes, both creep strength and fracture resistance are evaluated from the same basic test, and the properties that are being measured are changing during the course of the test. This test would be acceptable if it reflected the operating condition of the component. However, most components experience non-steady stresses and temperatures,

multiaxial stresses, cyclic stresses, active and often aggressive gaseous environments, and synergistic interactions among these factors.

With these deficiencies in mind, an alternative approach to testing and evaluation has been developed. The principal features of this design for performance methodology may be summarized as follows:

- Creep strength and fracture resistance are de-coupled and measured in separate tests or as distinctly different properties
- Both properties are measured as current values so that time-dependent changes during the test are minimal
- Creep strength is evaluated in terms of creep rate rather than time
- Fracture resistance is evaluated in terms of crack extension or ductility rather than time to failure
- State of damage is assessed in terms of current values of the critical properties

The following are examples of SRT derived creep rate data versus conventional creep rate (Woodford, 1993).

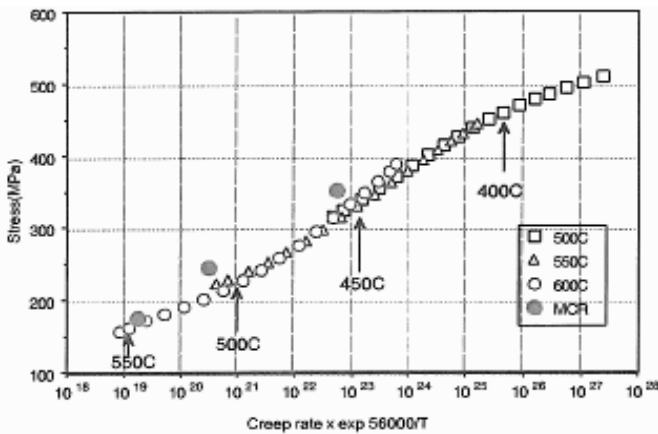


Figure 8. Creep Rate Parameter Comparison for Cr-Mo-V.

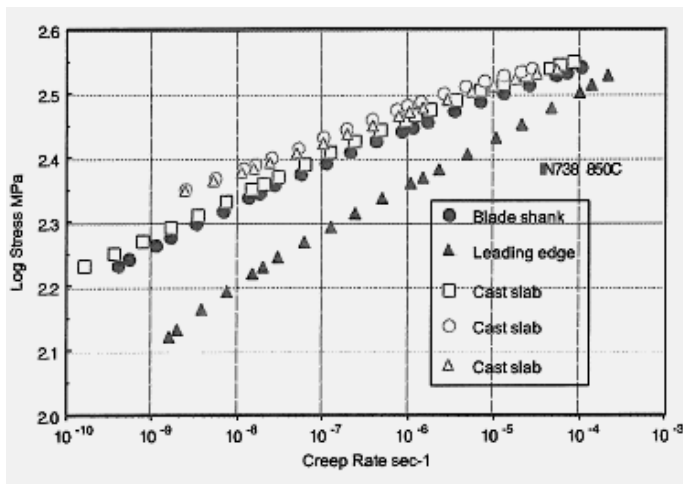


Figure 10. Stress vs. Creep Rate for Different Microstructures in IN738.

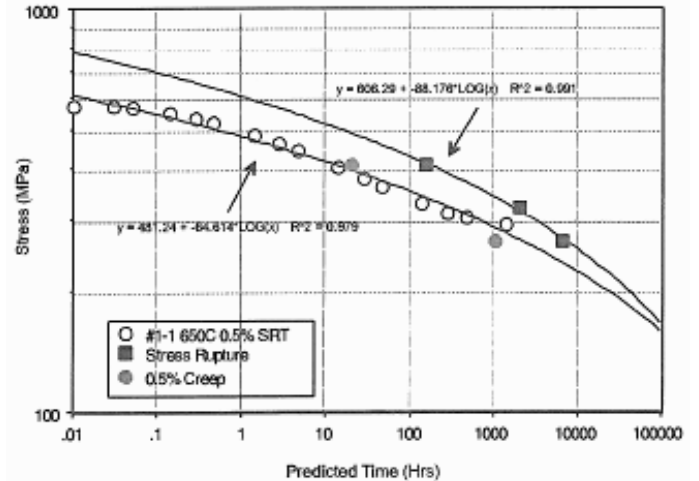


Figure 11. Projected Times TO 0.5% Creep FOR A286 at 650°C Compared with Actual Times for 0.5% Creep and Rupture.

Constant Displacement Rate Test

A description of the standardized CDR test is found elsewhere (Pope and Genyen, 1989). The data from the CDR test are tabulated in a curve similar to the load displacement curve for an ordinary elevated tensile test. For a typical tensile test fracture becomes unstable after the peak load is reached. On the other hand, in the CDR test, since the deformation is controlled at a constant rate and the notch is midway between the controlling extensometer, fracture rarely becomes unstable.

For a valid CDR test, the criteria for failure was considered to be the value of “displacement at fracture” defined as the point of intersection of the 100 pound load line and the descending load displacement curve. The “displacement at failure” is measured from the start of the test to the point where the load displacement curve decreases below 100 pounds (Figure 12).

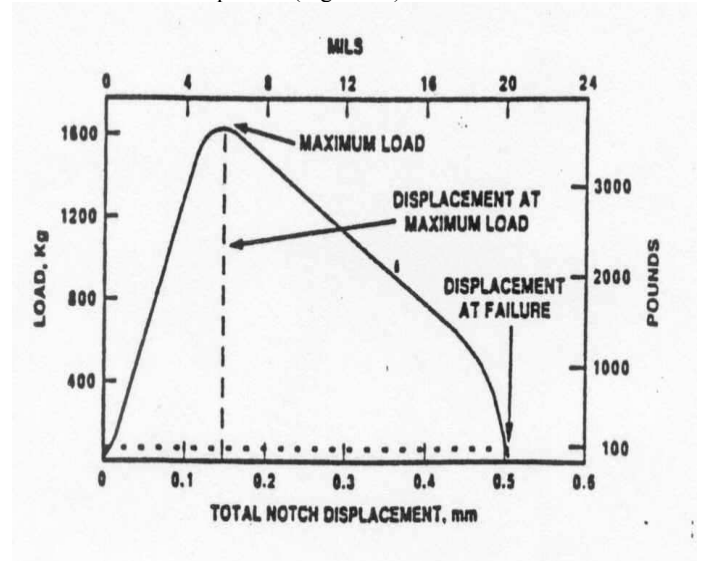


Figure 12. Example of Load Displacement Curve from CDR Tests at 1200°F and 2 mils/in/hr.

An example of how the environment can affect the notch sensitivity of the material is indicated by Figure 13. This example illustrates the effect of air exposure on IN738.

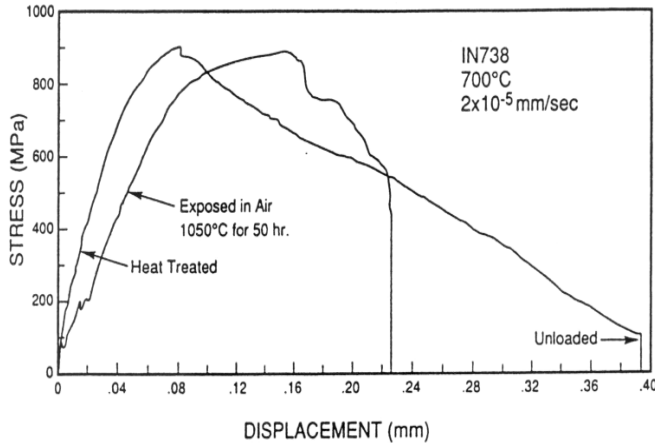


Figure 13. Constant Displacement Rate Tests Comparing Crack Growth Resistance in Heat Treated and Oxygen Embrittled Specimens.

Stress Relaxation Test

Specially designed samples were tested on an electromechanical test system fitted with self-aligning grips, a 1500°C (2732°F) short furnace, and a capacitive extensometer. Details of the specimen geometry and extensometer sensitivity are provided elsewhere (Woodford, et al., 1992).

The standard test procedure involved loading the specimen at a fast rate of 10 MPa/sec (1450 psi/sec) to a prescribed stress and then switching to strain control on the specimen and monitoring the relaxation stress. The inelastic (principally creep) strain-rate is calculated from the following equations, Equations (3) and (4).

$$\epsilon_e + \epsilon_l = \epsilon_t = \text{Constant} \tag{3}$$

$$\dot{\epsilon}_l = -\dot{\epsilon}_e = -\frac{1}{E} \frac{d\sigma}{dt} \tag{4}$$

where:

ϵ_e is the elastic strain, $\dot{\epsilon}_e$ is the elastic strain rate, ϵ_l is the inelastic strain (principally creep strain), $\dot{\epsilon}_l$ is the inelastic strain rate, ϵ_t is the total strain, σ is the stress, and E is the elastic modulus measured during loading. Using this procedure, stress versus strain-rate curves were generated covering up to five orders of magnitude in strain-rate in a test lasting less than five hours.

An example of the data generated in such tests is provided in Figure 14 for Waspaloy® material. This shows stress versus predicted time to one percent creep for Waspaloy®. By utilizing this data one can plot a stress versus Larson-Miller parameter for one percent predicted creep of Waspaloy® compared to rupture data (Figure 15). From the data shown on the curve, the stress relaxation test can generate creep-stress rupture data in less than a few weeks as compared to the traditional approach which incorporates long time testing.

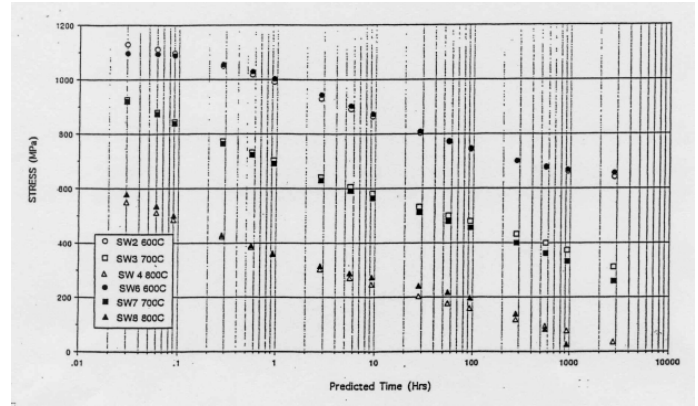


Figure 14. Stress vs. Predicted Times to 1% Creep for Standard Waspaloy.

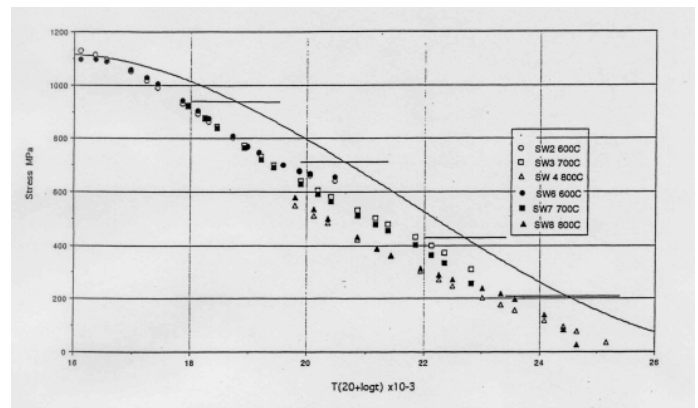


Figure 15. Stress vs. Larson-Miller Parameter for 1% Predicted Creep of Standard Waspaloy Compared with Rupture Data.

One major objective to this framework has been that effects of very long time exposures that could influence stress rupture life will not be accounted for. However, Woodford (1993) believes that such effects, i.e., precipitation of embrittling phases and grain boundary segregation of harmful elements, are expected to influence the fracture resistance rather than creep resistance. The authors’ company has utilized this methodology to generate data for high temperature materials and weldments. Current methods are being developed for miniature specimens taken from serviced blades. From these data, it is envisioned that establishment of a set of minimum performance criteria which will enable repair/rejuvenation/replacement decision to be made.

CREEP/FATIGUE INTERACTION

For components that operate at higher temperature where creep growth can occur, one must take into account of the creep crack growth at intervals during the fatigue life of the component. The following is an example of a high temperature steam turbine rotor that failed catastrophically at a power plant in Tennessee (Saxena, 1998). Further discussion of fracture mechanics concepts can be found elsewhere (Dowson, 1995, 1994). The authors utilized the latest computer software to demonstrate how creep-life, fatigue life, and creep/fatigue-life calculations can be performed, and how inaccurate the calculation would be without accounting the creep life.

The power plant was operated for 106,000 hours and had incurred 105 cold starts and 183 hot starts. The material was 1CR-1Mo-0.25V

forging and had been operating at a temperature of 800°F. The cracks originated from several majority node set (MnS) clusters with the original flaw size of 0.254 inch x 5.51 inch and 0.7 inch from the bore of the rotor (Figure 16). The bore temperature range was approximately 413-427°C.

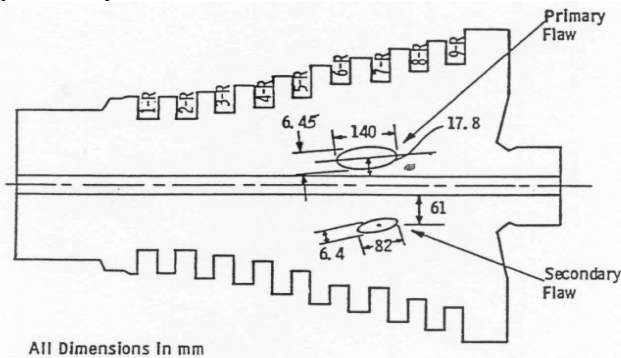


Figure 16. Schematic of the Intermediate Pressure (IP) Section of the Rotor Showing the Size and Location of the Primary and Secondary Flaws Beneath the Seventh Row (7-R) of Blades.

Assessment of low cycle fatigue life

The principle is that fatigue crack growth follows equation such as the Paris law:

$$\frac{da}{dN} = C_f \Delta K^{n_f} \tag{5}$$

C_f and n_f are constants that depend on the material and environment.

The stress intensity factor range ΔK depends on the stress level at the crack tip. The life assessment criteria is that critical crack size a_c is not to be exceeded. In other words,

$$a \leq a_c \tag{6}$$

By computing the information a plot of stress intensity factor versus crack depth was done using a pc CRACK LFM module. Based on the plane strain fracture toughness (K_{Ic}) of the material, the critical crack size 0.42 inch for cold start and 0.48 inch for hot start were determined (Figure 17).

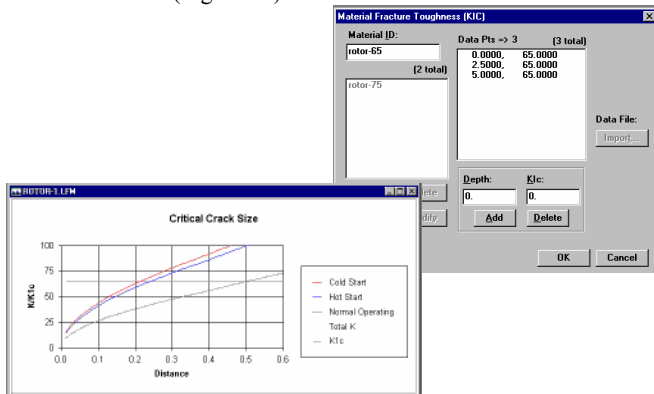


Figure 17. Critical Crack Size Calculation: The Critical Crack Size a_c is 0.42” for Cold Start and 0.48” for Hot Start.

Fatigue crack growth using the Paris law was computerized and the low cycle fatigue crack growth was determined for both cold and hot starts. Figure 18 shows the low cycle fatigue crack growth, which does not compare very well with that of the real life.

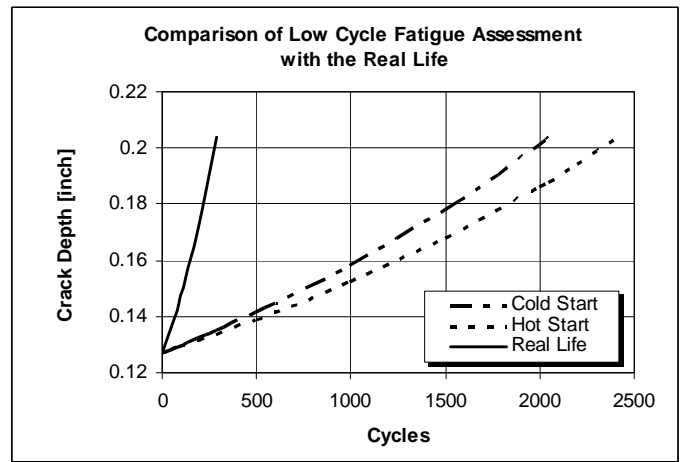


Figure 18. Shows Low Cycle Fatigue Crack Growth for Cold and Hot Starts Compared to Real Life.

The reason for the calculated life being much longer than the real life is that the hold time effect (or creep cracking effect) is not taken into account. Consequently, one must run a creep-fatigue remaining life assessment. The principle is that high temperature crack propagation is the summation of high temperature fatigue plus primary creep plus secondary creep.

Creep-Fatigue Crack Growth

$$\frac{da}{dt} = \underbrace{C_c [C_c(t)]^q}_{\text{Creep}} + \underbrace{\frac{C_f}{h} (\Delta K)^{n_f}}_{\text{Fatigue}} \tag{7}$$

where:
h is the hold time in each cycle (which is 368 hours in this case).

The creep crack driving force is consisted of two parts, which is based on Saxena’s relations considering the rate of growth of the creep zone in front of the crack (Saxena, 1986) as modified by Bloom and Malito (Bloom 1992).

$$C_c(t) = \underbrace{[C^*]^{2/(1+p)} \left[\frac{(1-\nu^2)K^2}{E(n+1)t} \right]^{1-2/(1+p)}}_{\text{Primary Creep}} + \underbrace{\frac{n+p+1}{(n+1)(p+1)} C_c^* \left(\frac{1}{t} \right)^{p/(p+1)}}_{\text{Secondary Creep}} + C^* \tag{8}$$

The elimination of primary creep is accomplished in Non-Linear Smart Crack by setting $m=n$ with inputs B_{1000} and p set to small values. The data that are input into the code is shown in Figure 19. The calculation shows that, accounting the creep effect, the creep-fatigue growth is much closer to the real life (Figure 20). By incorporating the creep crack growth C^* into the creep fatigue crack growth calculation, the total calculated cyclic life is closer to the actual cyclic life. Consequently, C^* can be the predominant crack growth parameter in the early stages of crack growth.

Materials Data	
Elastic Modulus, E	25000
Poisson's Ratio	.3
C (fatigue)	7.177E-10
n (fatigue)	2.7
A1000	2.1E-19
B1000	6.2E-15
n (creep)	7.3
m	2.43
P	2
Q'	73017
C (Creep coeff)	.000051
q (Creep exponent)	.6

Figure 19. Creep/Fatigue material Data.

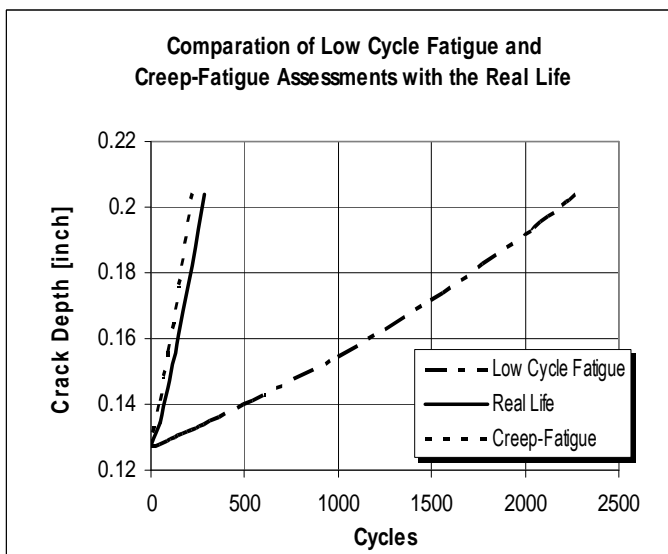


Figure 20. Compares Low Cycle Fatigue and Creep-Fatigue Crack Growth to the Real Crack Growth.

This example demonstrates that if the material/component is operating in the creep mode, one must perform a creep-fatigue analysis instead of fatigue only. Generally a rule of thumb is that if only low cycle fatigue crack growth is counted and creep is not, then the calculated lifetime is about 10 times longer than the real life. By utilizing this software program, more accurate remaining life assessment can be achieved for materials operating in the creep regime under cyclic loading. Also, the lesson being learned is that this rotor should have been examined by ultrasonic inspection every five years.

HIGH TEMPERATURE CORROSION

Fluid catalytic cracking (FCC) hot gas expanders operate in environments that can be both corrosive and erosive. Although it is well documented that the source of erosion comes from the regenerated catalyst that is carried with the hot flue gas from the FCC,

its effect on high temperature corrosion has only begun to be understood by the authors' company. Papers published by the author outline the relationship of stress and temperature on the high temperature corrosion/fracture mechanics of Waspaloy® in various catalyst environments (Dowson, et al., 1995, Dowson and Stinner, 2000).

The nature of the corrosion attack is primarily influenced by the type of crude oil stock, which in time has a bearing on the resulting flue gas composition, regenerated catalyst, and the nature and quality of additions injected into the FCC process.

When evaluating remaining life assessment of hot gas expanders especially the rotating components, one must consider the effect of the environment such as high temperature corrosion. The authors' company has developed a fracture mechanics model that incorporated both the effect of oxide wedge formation and the apparent reduction in fracture toughness of Waspaloy® in contact with the catalyst residue. By utilizing this model one can predict whether fracture will occur under various environmental/operating conditions of the hot gas expander. The authors' company periodically tests catalysts from end-users' hot gas expanders to determine if oxide wedge can occur and what life span to reach the critical size for failure. Generally, if the catalyst is active, then high temperature corrosion will occur. Consequently, a blade will be removed from the unit and examined metallographically to determine the oxide wedge depth. Based upon the depth and time of operation, the remaining life can be estimated (Figure 21). The short term catalyst test results generate the K_{IHTSCC} (initial fracture toughness at which crack growth can occur due to sulfidation).

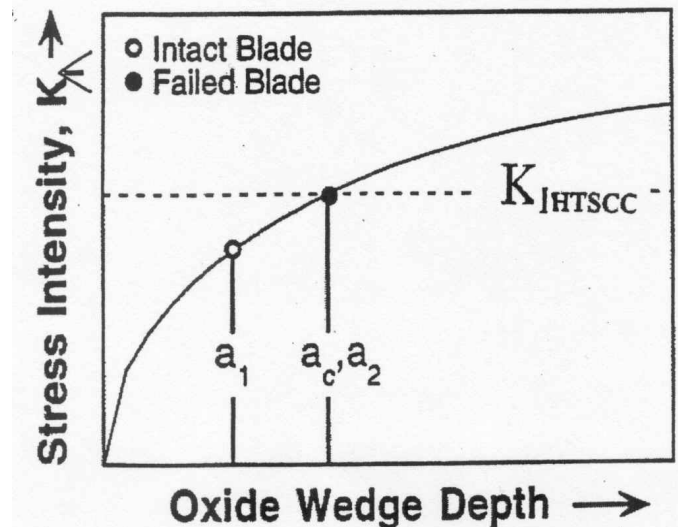


Figure 21. Stress intensity profile vs. oxide wedge depth for unit A. Critical oxide wedge depth for failure was defined as a_c . In the failed blade, a_2 was found to exceed a_c . In an intact blade, a_1 was less than a_c .

CASE STUDY

A life assessment was performed on a TH140 power recovery unit for both the disk and rotating Waspaloy blades. The unit had been in continuous operation for 10 yrs, accumulating approximately 85,000 hrs. The operational data revealed that the unit has run with a inlet temperature of 1296°F with only one afterburn where the temperature reached 1476°F for 3 days.

This life assessment consisted of:

- a) Testing of modified stress rupture specimens in the presence of FCC unit catalyst in order to determine if the species trapped in the catalyst were hazardous to the expander disk and blades.
- b) Corrosion testing
- c) Perform microstructural evaluation of both the disk and blades root locations using replication technique
- d) Hardness reading at both blade and disk root at both inlet and exhaust faces.
- e) Two blades were destructively tested to perform stress rupture, stress relaxation testing, constant displacement rate testing and evaluate evidence of high temperature corrosion attack. One of the blades was resoled and aged so that the results could be compared against the blade in the serviced condition. The blades removed from the disk were the original blades and had seen approximately 85,000 hrs.

a) Catalyst Corrosion Testing

In the present investigation a number of tests were done at stress levels of 75 ksi and at a temperature of 1350°F. Results varied with some bars failing before 5 hrs while others did not. Four Waspaloy rupture specimens W1-W4 were tested. Two failed while the other two did not (Table 4).

Table 4. Waspaloy Test Results

Specimen ID	Catalyst	Load [ksi]	Temp. [°F]	Duration	Status	Failure Location	Failure Mode	Fracture Morphology	Corrosion Wedge
W1	C1 (V-17)	70	1292	40 min	<i>failed</i>	at notch	corrosion-rupture	intergranular	Yes
W2	Air	70	1292	100 hrs	intact				
	C3 (V-17)			30 hrs	intact				
	C5 (V-66)			7.2 min	<i>failed</i>				
W3	C5 (V-66)	70	1100	5 hrs	intact	(The specimen was sectioned for examination.)			No
			1292	5 hrs	intact				
			1292	24 hrs	intact				
W4	C6 (V-66)	70	1292	18 hrs	intact	(This specimen was not sectioned.)			Not being examined
				17.5 hrs	intact				
				6.5 hrs	intact				
	C5 (V-17)			23 hrs	intact				
	C3 (V-17)			21 hrs	intact				

Both W1 & W2 fractures were examined using a scanning electron microscope (SEM) and the morphology was found to be intergranular for both fractures (Fig. 22-24). Corrosion wedges were found on the surface at the notch of both specimens (Fig. 25).

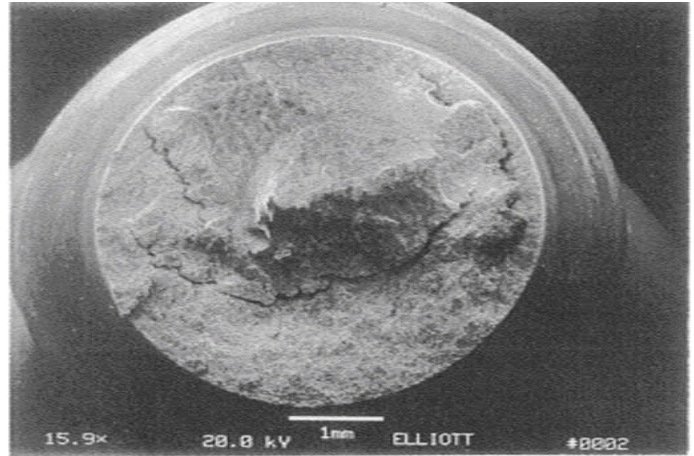


Figure 22 of Specimen W2

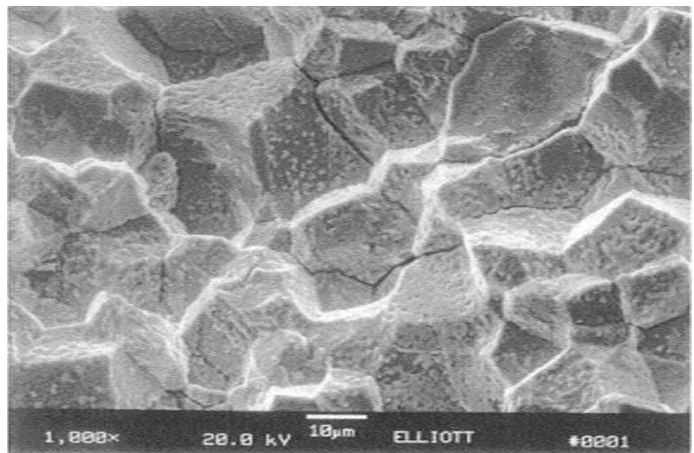


Figure 23 SEM of Specimen W2 with dominant intergranular feature

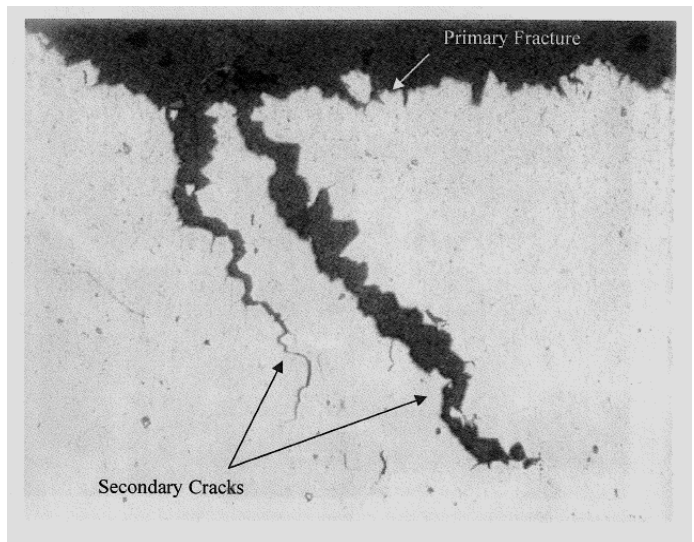


Figure 24. Cross-section of the fracture of specimen W2. Intergranular secondary cracks, located near the center of axis, were evident.

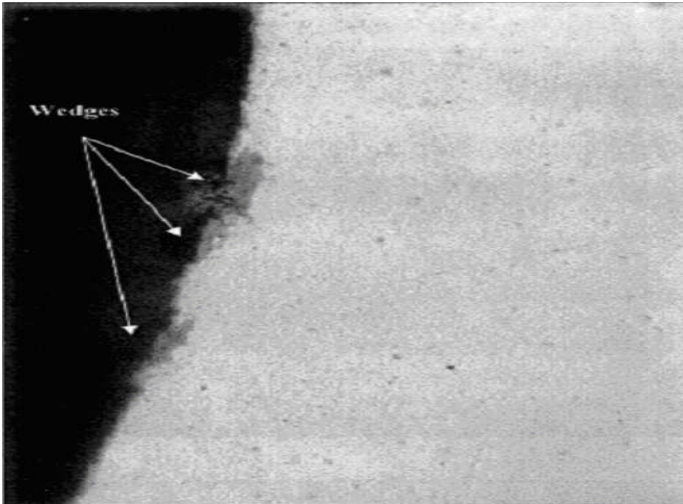


Figure 25. Cross-section of specimen Note the sulfidation corrosion wedges found on the notch surfaces where the stress was concentrated.

SEM/EDS indicated that the corrosion product was sulphide. This sulphide evidence is a strong indication of high temperature sulphidation corrosion.

Figure 26 shows setup for catalyst test.

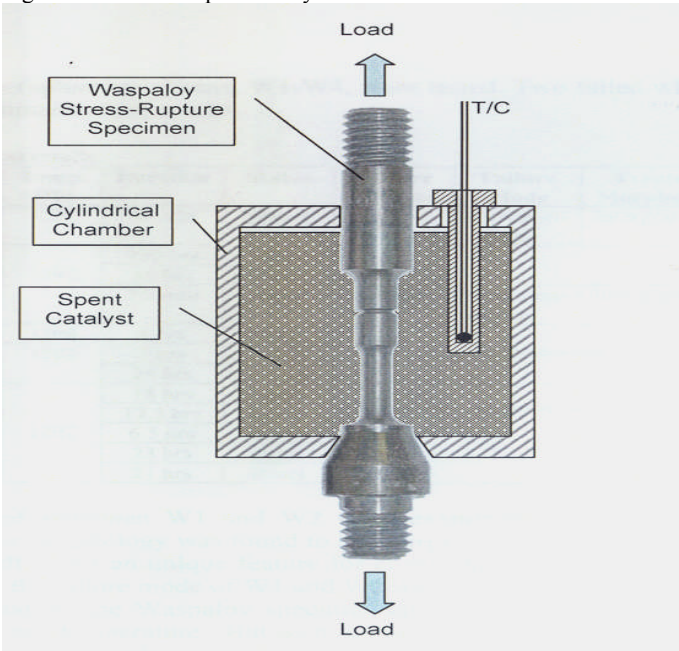


Figure 26. Setup of Stress-Rupture Rig for Catalyst Testing

Since the results were inconclusive that the spent catalyst was contaminated further destructive tests were performed in the blades such as SRT and CDR.

b) Corrosion Testing

The depth of the corrosion product was measured by taking cross-sectional samples along the top inside radius of the blade root. The five samples were mounted and polished for examination under an optical microscope. Corrosion wedges, as seen in Figure 27 were found along this inside radius. The deepest corrosion wedge found at

any location along this inside radius is shown in Figure 27, and depth of the corrosion wedge is 0.0043 inches (4.3 mils).

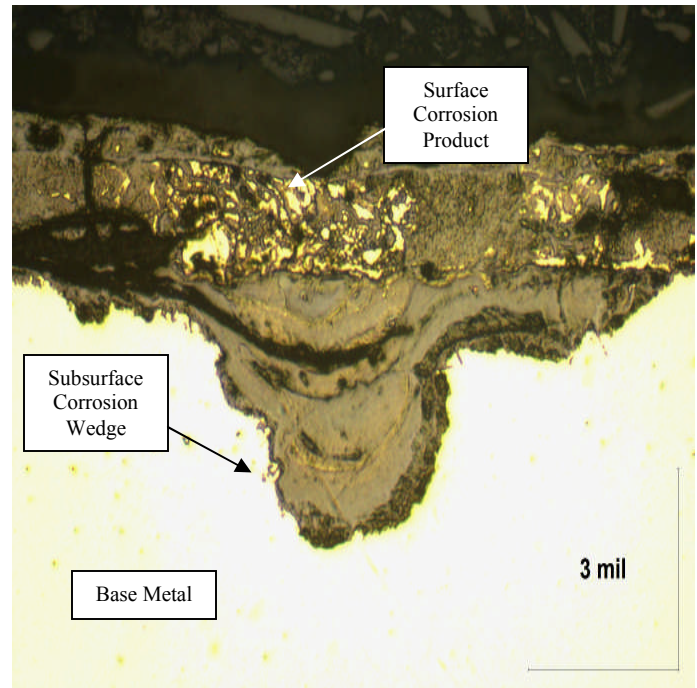


Figure 27. Photomicrograph of deepest corrosion wedge found in the blade root

Using a Scanning Electron Microscope (EDS), Energy Dispersive Spectroscopy (EDS) was performed on the corrosion product. The results of the EDS analysis indicate that the corrosion product on the surface of the Waspaloy is Nickel Oxide and Nickel Sulfide while the subsurface corrosion product is Chromium Oxide and Chromium Sulfide. These corrosion products are common in Nickel-based alloys which are under stress in environments containing both Oxygen and Sulfur.

The rate controlling operation in the high temperature corrosion process on the disk roots is the diffusion of ions through the oxide layer that has formed. When diffusion is the rate controlling step, the depth of the corrosion wedge will increase at a parabolic rate determined by the equation below.

$$X^2 = [k_p * t] / 2 \quad (9)$$

In this equation, X is the depth of the corrosion wedge, t is the time, and k_p is the parabolic rate constant. Knowing the maximum corrosion wedge depth is 4.3 mils after approximately 85,000 hours of operation, the constant k_p for this equation is 4.35×10^{-4} mils²/hour.

c) Hardness Testing

Hardness readings were taken on both the inlet and exhaust faces of the disk root (Table 5). The hardness readings were consistent at all locations on both faces of the disk and met the requirements of the authors' Waspaloy material specification. This evidence indicates that the disk material had not been exposed to excessive heat during operation.

Table 5. Average Hardness Values at Examined Disk Locations

	Inlet Face	Exhaust Face
Tip of Disk Root	37.7 HRC	38.2 HRC
Base of Disk Root	39.4 HRC	40.9 HRC
Disk Body	39.8 HRC	40.1 HRC

d) Microstructural Evaluation

Replicas of the microstructure of the disk were taken from 10 locations shown in Fig 28 and subsequently examined by an optical microscope.

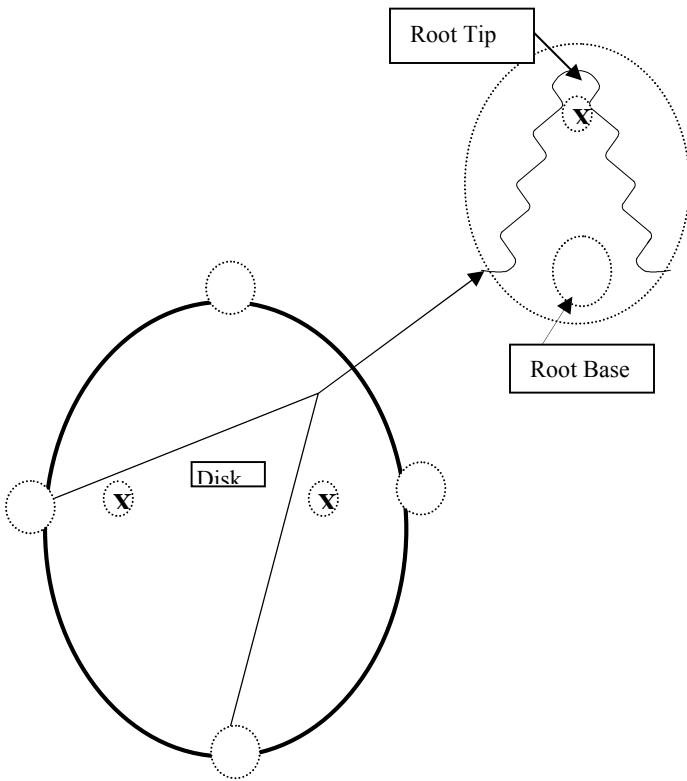


Figure 28. Diagram illustrating the locations of the disk from which replicas were taken. All 10 areas were examined on both the inlet and exhaust faces of the disk

The replicas were a rubber like resin substance attached to backing paper. The microstructures of the replicas, shown in Fig. 29-31, are consistent at all locations on both the inlet and exhaust faces of the disk. The average grain size at all locations on the disk is ASTM 5.5 and conforms to the requirements of the authors' Waspaloy material specification. This is further evidence that the disk material was not exposed to excessive heat during operation. The microstructure indicated there was not evidence of cavitation creep damage as there were no voids at the grain boundary triple points.

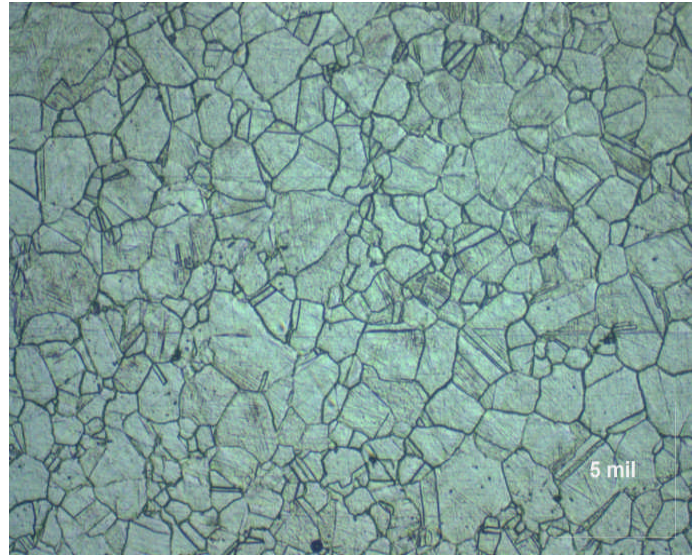


Figure 29. Inlet Face – Tip of Disk Root

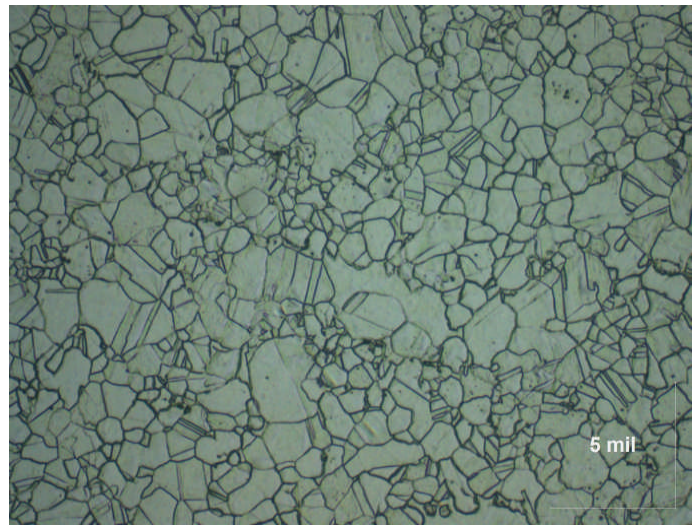


Figure 30. Exhaust Face – Tip of Disk Root

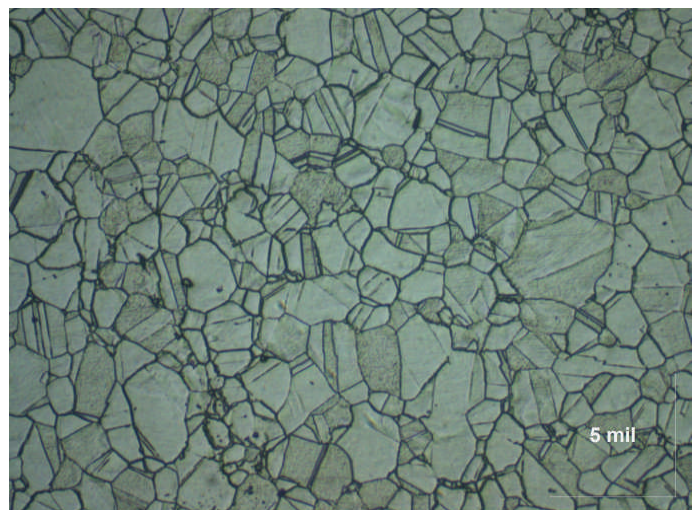


Figure 31. Inlet and Exhaust Face

e) Blade Examination

Two of the Waspaloy blades that had seen 85,000 hrs were taken out of service for destructive testing. One of the blades was resolution treated and aged in accordance to the authors' Waspaloy heat treatment procedure and sectioned for mechanical and metallurgical examination. The other blade referred to "as service condition" was tested in a similar manner to the reheat treated blade.

Sections from the root of the "as service condition blade" and the "reheat treated blade" were sectioned and polished for examination under an optical microscope. Photomicrographs of the microstructure of these blade roots are shown in Fig. 32 & 33. The photomicrographs show that the average grain size of both blade roots is ASTM 4 which is slightly larger than the average grain size of the disk, however, this grain size still meets the authors' material specification requirements. Again, no evidence of cavitation creep damage or exposure to temperatures beyond the designed service temperature could be found.

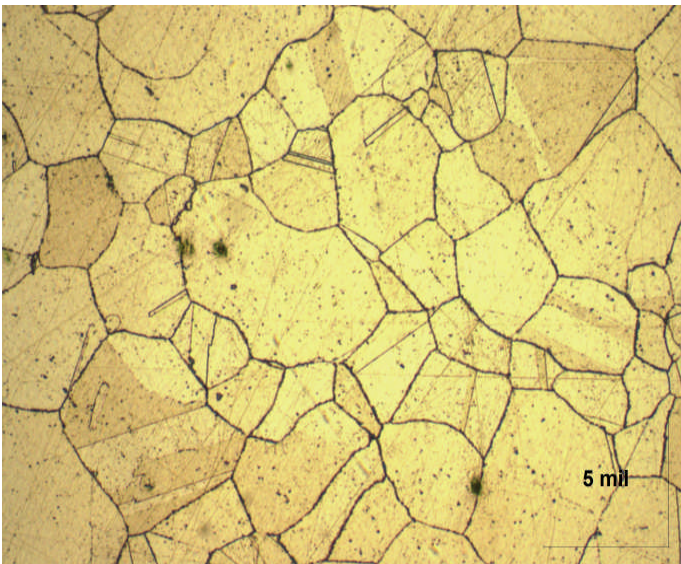


Figure 32. Photomicrograph of Service Condition Blade Root

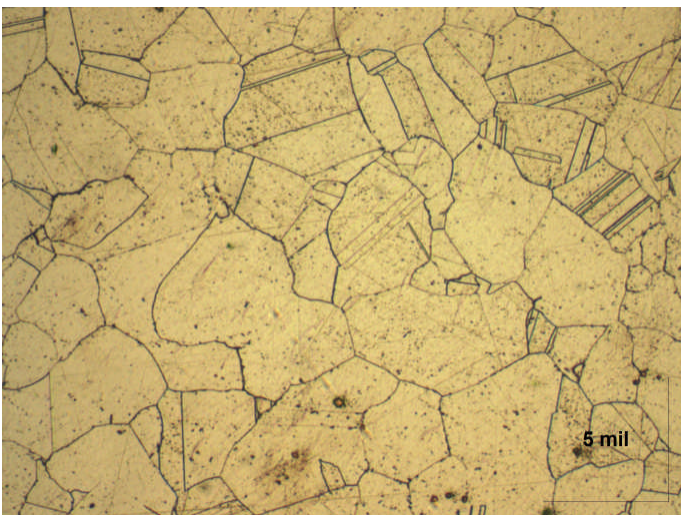


Figure 33. Photomicrograph of Re-Heat Treated Blade Root

There is a slight difference between the grain boundaries of the as-service blade and the re-heat treated blade under higher magnification. The grain boundaries of the service condition blade, shown in the photomicrograph in Figure 34, reveal that the carbides at grain boundaries are not completely discrete at all locations. There is also evidence that carbides are precipitating at the grain boundaries. These observations are illustrated by comparison to the microstructure of the re-heat treated blade, which is shown in the photomicrograph in Figure 35. The grain boundaries of the re-heat treated blade are more discrete and there are fewer precipitates present at the grain boundary locations.

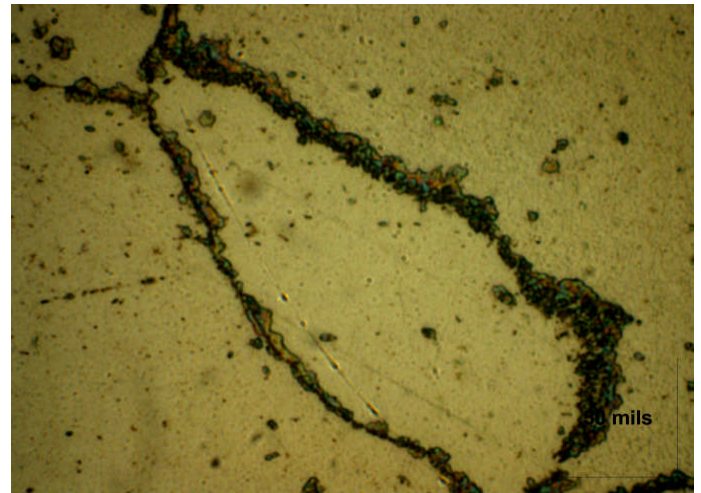


Figure 34. Photomicrograph of Grain Boundary on Service Condition Blade Root

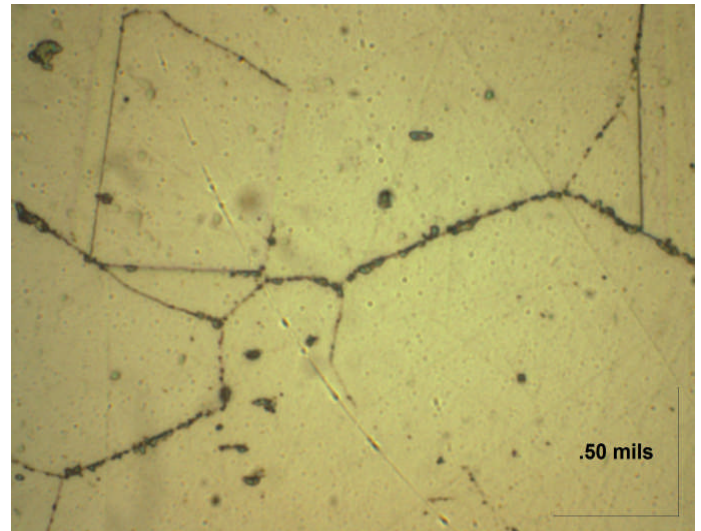


Figure 35. Photomicrograph of Grain Boundary on Re-Heat Treated Blade

Stress Rupture Testing

Stress rupture testing was performed on samples taken from service condition blades as well as the reheat treated blade root. The stress rupture bars were standard smooth/notch bars in accordance with ASTM E292 specimen #4. The results of the stress rupture testing are shown in Table 6.

Table 6. Stress Rupture Testing

Stress Rupture Testing 1350°F at 75,000 psi stress			
	Time to Fracture	% Elongation	Fracture Location
Service Condition Blade	40.44 hours	23%	Smooth
Reheat Treated Blade	70.34 hours	9%	Smooth

Experimental Procedure and Results

Standard tensile specimens taken from both the service condition blade and the re-heat treated blade were taken for SRT and CDR testing. The SRT test specimens had a 1 inch gauge length and were 0.160 inches in diameter. The CDR test specimens had the same dimensions with a 60° notch in the center of the gauge length. The test matrix is given below. Samples tested under similar conditions, such as SRT 1 and SRT 4, were taken from identical locations in both the service condition blade and the re-heat treated blade (Table 7).

Table 7

Service Condition Blade	
SRT 1	SRT from 0.4% total strain and 1.3% total strain at 600°C
SRT 2	SRT from 0.4% total strain and 1.3% total strain at 700°C
SRT 3	SRT from 0.4% total strain and 1.3% total strain at 800°C
CDR1	600°C
CDR 2	650°C
Re-Heat Treated Blade	
SRT 4	SRT from 0.4% total strain and 1.3% total strain at 600°C
SRT 5	SRT from 0.4% total strain and 1.3% total strain at 700°C
SRT 6	SRT from 0.4% total strain and 1.3% total strain at 800°C
CDR 3	600°C
CDR 4	650°C

The strain levels of 0.4% total strain and 1.4% total strain were selected to so that the SRT tests would be conducted just beyond the elastic limit of the material and at a plastic strain of 1%. This testing produces comparative relaxation data for the unrestrained condition at 0.4% total strain and a comparison basis with long time creep data to 1% creep strain at 1.4% total strain.

The test procedure involved loading the SRT tests to the prescribed strain levels and holding at that strain for 20 hours at temperature. During the holding time, the stress relaxes as the elastic strain is replaced with inelastic creep strain. After holding for 20 hours, the stress on the samples was reduced to approximately 1.5 ksi and held constant for 2 hours while the samples contracted due to recoverable time-dependant anelastic strain. The stress at various times during the relaxation of the samples was recorded.

Using the elastic modulus of the material which was measured during the loading of the test, the stress vs. time response was fitted with a fourth order polynomial which was differentiated to convert to a stress vs. creep rate curve. The data obtained from this testing covers approximately five decades of time. From the stress vs. creep rate curves, the time required to induce 1% creep on the material was calculated.

Using the estimated times for 1% creep, a Larson-Miller parameter curve was constructed. This curve is shown in Figure 36. The Larson-Miller curves again demonstrate the slight reduction in creep strength of the service-condition material in comparison to the re-heat treated material for the 600°C and 700°C samples.

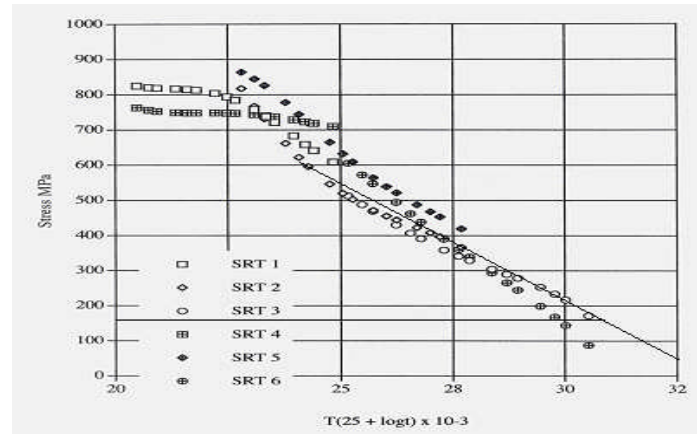


Figure 36. Stress vs. Larson Miller Parameter for 1% Creep of Service Condition Blade and Re-Heat Treated Blade (Legend Defined in Table 7)

Figure 37 gives a comparison of the creep rate curves at various stresses for both the re-heat treated material and the service condition material against standard Waspaloy samples. As seen in Figure 37, although the creep rate curves of the service condition material is lower than that of the re-heat treated material, the creep rate curves of the service condition material is approximately the same as the standard Waspaloy samples at 600°C and 700°C and even higher than the standard samples at 800°C.

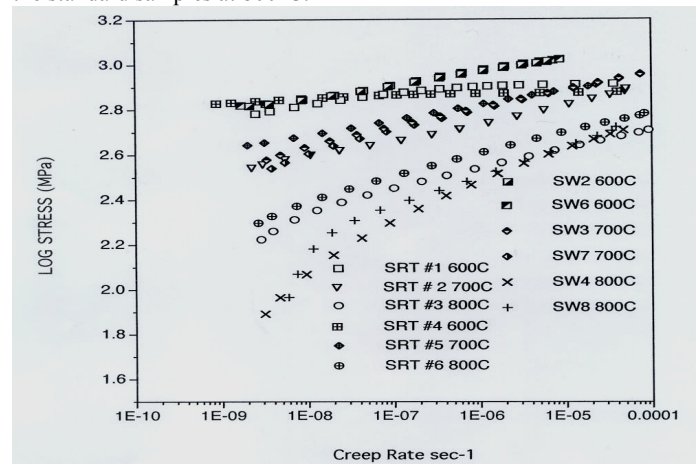


Figure 37. log Stress vs. Creep Rate Curves Comparing the Service Condition Blade and the Re-Heat Treated Blade with Standard Waspaloy Samples (SW) (Legend Defined in Table 7)

The test procedure for the CDR specimens involved heating the samples to 600°C and 650°C because Waspaloy material displays a ductility minimum at these temperatures. A constant displacement rate of $7 \times 10^{-5} \text{ mm} \cdot \text{sec}^{-1}$ was then applied. The displacement across the notch at the time of fracture and the amount of unloading before the fracture both give a measurement of the fracture resistance of the material. Stress readings were taken at 1 second intervals for these tests, and the amount of unloading recorded is a measure of the crack size prior to fast fracture. The results of this testing for both the re-heat treated samples and the service condition samples are given in Figure 38.

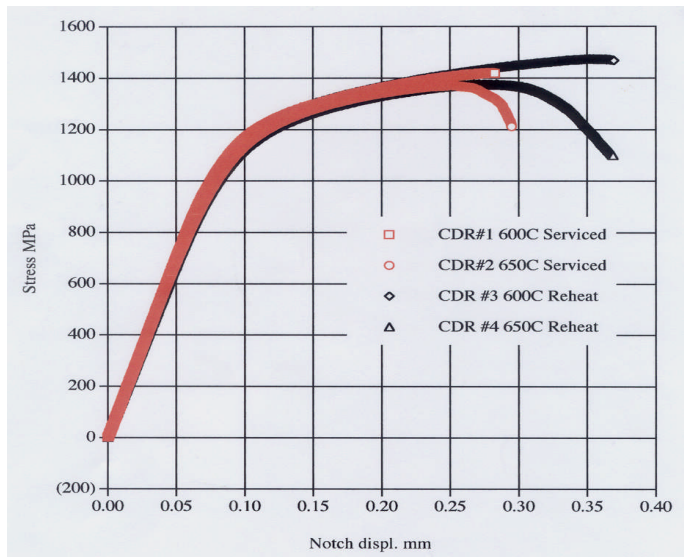


Figure 38. CDR Results at 600°C and 650°C for Service Condition Blade and Re-Heat Treated Blade (Legend Defined in Table 7)

It is clear from the results in Figure 38 that the re-heat treated material has significantly greater notch displacement at the time of fracture than the service condition material at both testing temperatures. The re-heat treated material also demonstrated a much greater amount of unloading at 650°C than the service condition material. The notch displacements of the re-heated material were comparable to standard Waspaloy samples. Although the service condition material has less notch ductility than the re-heat treated material, stress rupture testing indicated that the service condition material is not notch sensitive as the stress rupture sample fractured in the smooth location.

Remaining Rupture Life

From the data generated during the Stress Relaxation Testing, a graph of Stress vs. Time to 1% Creep was obtained. This graph provides stress rupture data from the service condition material and can be used to determine the remaining stress rupture life of disk.

The SRT testing of the service condition material was performed at 600°C, 700°C and 800°C, yielding Stress vs. Predicted Time to 1% Creep data at these three temperatures. The average inlet temperature of the unit was reported to be 1297°F (702°C). Using the SRT data for the service condition material at 700°C along with a very conservative value of a 160 MPa for the mean stress at the disk root, the disk will reach 1% creep after 3×10^6 hours of operation. This disk has currently experienced 85,000 hours of operation, which is only 3% of the 1%

rupture life. Since this calculation was based on the inlet temperature of the unit, the time to 1% creep is an extremely conservative value because the disk root will be exposed to lower temperatures than the inlet temperature.

Only one significant afterburn was reported by the customer, where the inlet temperature of the expander reached 1467°F (797°C) for 3 days. By using the Stress vs. Time to 1% Creep data service condition material tested at 800°C and using the same conservative mean stress value at the disk root, a time of 2,340 hours is necessary before the disk experiences 1% creep deformation. The disk may have seen this temperature for up to 72 hours, which equals 3% of the 1% rupture life under these conditions. Again, this is a very conservative value since the expander disk root will be exposed to a lower temperature than the inlet temperature. By using the Life Fraction Rule which states the fraction of the remaining rupture life used up under various conditions may be added up to determine to total amount of rupture life that has been expended, a total of 6% of the 1% creep rupture life of the disk has been used.

Conclusions & Recommendations

Examination of the disk microstructure taken from replicas reveal a consistent grain size between the disk roots and the body of the disk on both the inlet and exhaust faces. No evidence of creep damage or exposure to temperatures beyond the service temperature could be found. The hardness at all locations was also consistent which provides further proof that the disk was not exposed to excessive temperatures.

Two blades were taken from the unit for further examination and destructive testing, and one of these blades was re-solution treated and aged before testing. A comparison of the microstructures between the blades shows a less discrete grain boundary of the service condition blade as well as possible evidence of precipitates forming at the grain boundaries. The re-heat treated blade had a longer time to rupture than the service condition blade during stress rupture testing, however, both blades meet the stress rupture requirements of Elliott MS-487A and both samples fractured in the smooth location.

Stress Relaxation Testing (SRT) showed that there has been a slight reduction in the creep strength in the service condition blade in comparison to the re-heat treated blade. The creep strength of the service condition blade still compares well to standard Waspaloy SRT samples tested under the same conditions at the service temperature of the unit. Constant Displacement Rate (CDR) testing reveals that the service condition blade does display a reduction in notch ductility in comparison to the re-heat treated blade, however the stress rupture test indicated that the material was not severely notch sensitive due to the failure occurring in the smooth section of the specimen.

Stress rupture testing in the presence of catalyst provided showed that the Waspaloy was not subject to corrosive attack by any impurities in the catalyst during the test.

Cross-sectional samples taken from the inside radius of the top blade root of the service condition blade revealed that a sulfide corrosion wedge had formed. This corrosion wedge had a depth of 0.0043 inches, and fracture mechanics performed on the blade root show that this corrosion wedge will not reach a critical depth of 0.150 inches during the life of unit if conditions remain constant.

The conclusion from the remaining life assessment testing is that the disk is suitable for future service under the current operation conditions of the unit. The current condition of the disk does not indicate a significant reduction in the creep strength of the material or any significant changes to the microstructure.

REFERENCES

- Bloom, J.M., and Malito, M.L., 1992, "Using C_1 to Predict Component Life", Fracture Mechanics: Twenty-Second Symposium (Volume 1), ASTM STP 1131, Philadelphia, Pennsylvania, pp. 393-411
- Bush, S.H., 1982, "Failures in Large Steam Turbine Rotors, in Rotor Forgings for Turbines and Generators," R.I. Jaffe, Ed., Pergamon Press, New York, p. I-1 to I-27.
- Carlton, R.G., Gooch, D.J., and Hawkes, B.M., 1967, The Central Electrical Generating Board Approach to "The Determination of Remanent Life of High Temperature Turbine Rotors," I. Mech E. paper C300/87.
- Dowson, P., 1994, "Fitness for Service of Rotating Turbomachinery Equipment," 10th Annual North American Welding Research Conference, Columbus, Ohio, October 3-5.
- Dowson, P., 1995, "Fracture Mechanics Methodology Applied to Rotating Components of Steam Turbines and Centrifugal Compressors," Third International Charles Parson Turbine Conference, Materials Engineering in Turbine and Compressors, Vol. 2, pp. 363-375.
- Dowson, P. and Rishel, D., 1995, "Factor and Preventive Measures Relative to the High Temperature Corrosion of Blade/Disk Components in FCC Power Recovery Turbines," *Proceedings of the 24th Turbomachinery Symposium*, Turbomachinery Laboratory, Texas A&M University, College Station, Texas, September, pp. 11-26.
- Dowson, P. and Stinner, C., 2000, "The Relationship of Stress and Temperature on High-Temperature Corrosion Fracture Mechanics of Waspaloy in Various Catalyst Environments," *Proceedings of High Temperature Corrosion and Protection, Materials at High Temperatures* 18(2), pp. 107-118.
- Fossati-Sampietri/CESI, 2001, "Determination of Remaining Life Prior to Successive Checks for a Component Subject to Creep," Seminar in Siracusa, Italy.
- Goldhoff, R.M. and Woodford, D.A., 1972, "The Evaluation of Creep Damage in CrMoV Steel in Testing for Prediction of Material Performance in Structure and Components," STP 515 American Society for Testing and Materials, Philadelphia, pp. 89-106.
- Neubauer, E. and Wadel, V., 1983, "Rest Life Estimation of Creep Components by Means of Replicas", *Advances in Life Prediction Methods*, Ed., Woodford, D.A., and Whitehead, J.E., (New York: ASME), pp. 307-314.
- Pope, J.J. and Genyen, D.D., 1989, *International Conference on Fossil Power Plant Rehabilitation*, ASM International, pp. 39-45.
- Saxena A., 1986, "Creep Crack Growth under Non-Steady-State Conditions", *Fracture Mechanics: Seventeenth Volume*, ASTM STP 905, Philadelphia, Pennsylvania, pp. 185-201
- Saxena A., 1998, "Nonlinear Fracture Mechanics for Engineers," Boca Raton, Florida, CRC Press, p. 449.
- Viswanathan, R. and Gehl, S.M., 1991, "A Method for Estimation of the Fracture Toughness of CrMoV Rotor Steels Based on Composition," ASME Transaction, *Journal of Engineering Mat. and Tech.*, Vol. 113, April, pp. 263.
- Viswanathan, R. and Gehl, S.M., 1992, "Life-Assessment Technology for Power Plant Components," *JOM*, February, pp. 34-42.
- Woodford, D.A., 1993, *Materials and Design*, Vol. No. 4, p. 231.
- Woodford, D.A., Von Steele, D.R., Amberge, K., and Stiles, D., 1992, "Creep Strength Evaluation for IN738 Based on Stress Relaxation" from *Superalloys*, The Minerals, Metals and Material Society, Editors, Antolovich, S.D., Stusned, R.W., Mackay, R.A., Anton, D.L., Khan, T., Kissinger, R.D., Klarstrom, D.L., pp. 657-663.
- Woodford, D.A., 1993, "Test Methods for Accelerated Development, Design and Life Assessment of High Temperature Material" *Materials & Design*, Vol. 14, pp. 231-242.